Quantum thermal transistor based on qubit-qutrit coupling

Bao-qing Guo, Tong Liu, and Chang-shui Yu*
School of Physics, Dalian University of Technology, Dalian 116024, China

(Received 9 June 2018; revised manuscript received 29 July 2018; published 20 August 2018)

A quantum thermal transistor is designed by the strong coupling between one qubit and one qutrit which are in contact with three heat baths with different temperatures. The thermal behavior is analyzed based on the master equation by both the numerical and the approximately analytic methods. It is shown that the thermal transistor, as a three-terminal device, allows a weak *modulation* heat current (at the modulation terminal) to *switch on and off* and effectively modulate the heat current between the other two terminals. In particular, the weak *modulation* heat current can induce the strong heat current between the other two terminals with the multiple-region *amplification* of heat current. Furthermore, the heat currents are quite robust to the temperature (current) fluctuation at the lower-temperature terminal within a certain range of temperature, and so it can behave as a heat current *stabilizer*.

DOI: 10.1103/PhysRevE.98.022118

I. INTRODUCTION

The diode [1] and the transistor [2], which directly led to the revolution of electronic information in the last century, are important components that realize the management of electronic transport. Diodes are two terminal electronic devices that guide the electric conduction based on the direction of the electric current, and transistors with three terminals utilize the electric current at one terminal to control the electric conduction between the other two terminals to realize three basic functions: a switch, an amplifier, or a modulator. In a similar manner, thermal devices were expected to be developed for the potential management of heat currents. It was shown in experiments that heat currents could be switched on and off in various materials such as carbon nanotube structures [3] and others [4–7], and similar functions for heat as the diode or the transistor were shown by VO_2 [8–13].

The increasing interest in quantum thermodynamics has paved the way for studying macroscopic thermodynamic laws at the quantum level and designing thermal machines or devices in quantum systems. For examples, the Fourier laws for heat conduction and the second thermodynamic law were studied in various systems [14–24], and a quantum heat engine and refrigerator [25–45] have also been designed. In particular, it has been shown that not only the heat logic gates [46], the thermal memory [47], the thermal ratchet [48,49], and the thermometer [50], but also the analogues of the electronic devices, the thermal rectifier [5,51–59], and the transistor [12,13,59–63] have been theoretically proposed and investigated extensively. It is worth emphasizing that thermal devices with only several levels have also been proposed, such as a thermal rectifier made of only one quantum dot with high in-plane magnetic fields [4], optimal rectification consisting of two two-level systems (TLSs) in a magnetic field [51], a quantum thermal transistor with three TLSs [60,64], and so on. Recently artificial atoms such as superconducting circuits and spins in solids [65,66] have provided a novel and flexible method to investigate quantum thermodynamics or to design quantum thermal machines [67,68]. In this sense, how to design the thermal device in the small system and how to improve the various performance indices of some particular functions have become the significant topics.

In this paper, we design a thermal transistor by employing only strong qubit-qutrit coupling. Our thermal transistor consists of one qubit and one qutrit which interact with three heat baths with different temperatures. The master equation governing the dynamic evolution of the open system is derived and solved numerically and approximately analytically. It is shown that our thermal transistor allows a weak *modulation* heat current to switch on and off and effectively modulate the heat current between the other two terminals. In particular, the weak *modulation* heat current can induce the strong heat current between the other two terminals, which realizes the typical function of a transistor—the amplification. Moreover, it is shown that the heat currents are quite robust to the temperature change at the lower-temperature terminal within a certain range of temperature, so it can be used to realize the heat current stabilization subject to the temperature fluctuation at the lower-temperature terminal. The distinct features of our transistor are (1) at the *off* state, the *modulation* heat current has a large allowable region and a quite weak heat current; (2) the transistor has multiple (stable or sensitive) amplification regions which have different (very large) amplification factors; and (3) it is robust to the temperature fluctuation at the lower-temperature terminal. The rest of this paper is organized as follows. In Sec. II we derive the master equation that governs that evolution of our proposed open system. In Sec. III we solve the master equation and calculate the heat currents at the steady state. In Sec. IV we analyze the thermal behavior and show how our system behaves as a quantum thermal transistor. Finally, discussion and conclusion are given in Sec. V.

II. THE MODEL AND THE DYNAMICS

Our model as sketched in Fig. 1, consists of a qubit as the *modulation* qubit which is in contact with a heat bath M with temperature T_M and simultaneously interacts with a *target*

*ycs@dlut.edu.cn

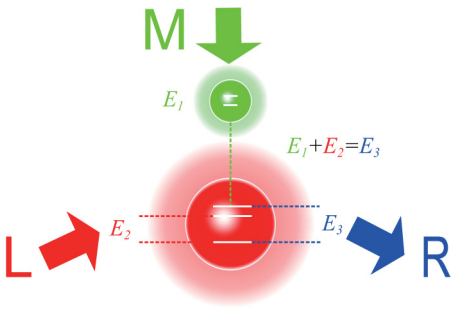

FIG. 1. A *modulation* qubit in contact with the heat bath M and a qutrit connected to the heat bath L and the heat bath R are strongly coupled with each other, which act as a quantum thermal device. The ground state and the first excited state of the qutrit are greatly separated, while the transition between the first and the second excited states is resonantly coupled to the *modulation* qubit.

qutrit which is in contact with a heat bath L and a heat bath R with their temperatures denoted by T_L and T_R, respectively. In the following, we will demonstrate that the weak heat current through the *modulation* qubit can be used to switch on and off, to modulate and stabilize the heat currents through the target qutrit from the L bath to the R bath (or in the opposite direction). In particular, as a key feature of the transistor, it can be seen that the amplification of the weak heat current can also be realized by this model.

To show this, let's turn to the dynamical procedure of our model. For simplicity, we would like to suppose that the ground-state energies are zero for both the qubit and the qutrit. Let $|1\rangle_1 = [1, 0]^T$ denote the excited state of the qubit with energy E_1 and $|1\rangle_2 = [0, 1, 0]^T$ and $|2\rangle_2 = [1, 0, 0]^T$ denote two excited states of the qutrit, respectively, corresponding to energies E_2 and E_3. In addition, we suppose the qubit and the qutrit interact with each other via the Hamiltonian

$$H_I = g(|11\rangle\langle 02| + |02\rangle\langle 11|) \tag{1}$$

with g representing the coupling strength, so the Hamiltonian of the bipartite interacting system reads

$$H_S = H_0 + H_I, \tag{2}$$

where the free Hamiltonian is

$$H_0 = E_1|1\rangle_1\langle 1| + E_2|1\rangle_2\langle 1| + E_3|2\rangle_2\langle 2|. \tag{3}$$

Here we consider the resonant coupling, i.e., $E_1 + E_2 = E_3$, and we set the Boltzmann constant and the Plank constant to be a unit, i.e., $\hbar = k_B = 1$. Now let's consider the qubit-qutrit system interacts with three heat baths which are described by the quantized radiation field. The free Hamiltonian of the three baths reads

$$H_\mu = \sum_k \omega_{\mu k} b^\dagger_{\mu k} b_{\mu k}, \mu = L, M, R, \tag{4}$$

where $\omega_{\mu k}$ and $b_{\mu k}$ denote the frequency and the annihilation operator of the bath modes, respectively, with $[b^\dagger_{\mu k}, b_{\nu k'}] = \delta_{\mu,\nu}\delta_{k,k'}$, $[b^\dagger_{\mu k}, b^\dagger_{\nu k'}] = 0$, $[b_{\mu k}, b_{\nu k'}] = 0$. The interaction Hamiltonian between the system and the baths is given by

$$\begin{aligned} H_{SB} = &\sum_k f_{Lk}(b^\dagger_{Lk}|0\rangle_2\langle 1| + b_{Lk}|1\rangle_2\langle 0|) \\ &+ \sum_k f_{Mk}(b^\dagger_{Mk}|0\rangle_1\langle 1| + b_{Mk}|1\rangle_1\langle 0|) \\ &+ \sum_k f_{Rk}(b^\dagger_{Rk}|0\rangle_2\langle 2| + b_{Rk}|2\rangle_2\langle 0|), \end{aligned} \tag{5}$$

where $f_{\mu k}$ denotes the coupling constants between the kth mode in the μth bath and the corresponding energy levels of the system. Thus the Hamiltonian of the whole open system can be given as

$$H_{\text{total}} = H_S + \sum_\mu H_\mu + H_{SB}. \tag{6}$$

Based on such a Hamiltonian (6), one can derive the dynamical equation of the open system, i.e., the master equation [69]. One can note that H_S can be diagonalized as $H_S = \sum_{i=1,2,\ldots,6} \lambda_i|\lambda_i\rangle\langle\lambda_i|$, where the eigenvalues are given by $|\lambda\rangle^T = [\lambda_1, \lambda_2, \ldots, \lambda_6] = [E_1 + E_3, E_3 - g, E_1, E_3 + g, E_2, 0]$, and the corresponding eigenstates are

$$\begin{aligned} &|\lambda_1\rangle = |12\rangle, \quad |\lambda_2\rangle = \frac{1}{\sqrt{2}}(|11\rangle - |02\rangle), \quad |\lambda_3\rangle = |10\rangle, \\ &|\lambda_4\rangle = \frac{1}{\sqrt{2}}(|11\rangle + |02\rangle), \quad |\lambda_5\rangle = |01\rangle, \quad |\lambda_6\rangle = |00\rangle. \end{aligned} \tag{7}$$

In the H_S presentation, the interaction Hamiltonian H_{SB} can be rewritten as

$$H_{SB} = \sum_{\mu,k,j} f_{\mu k}[b^\dagger_{\mu k} V_{\mu l}(\omega_{\mu l}) + b_{\mu k} V^\dagger_{\mu l}(\omega_{\mu l})],$$

where $V_{\mu l}(\omega_{\mu l})$ stands for the eigenoperator of H_S corresponding to the eigenfrequency $\omega_{\mu l}$ with the relation $[H_S, V_{\mu l}(\omega_{\mu l})] = -\omega_{\mu l} V_{\mu l}(\omega_{\mu l})$. The concrete expressions of the eigenoperators are given in Appendix A. It is clear that the transitions $|\lambda_3\rangle \leftrightarrow |\lambda_2\rangle$, $|\lambda_6\rangle \leftrightarrow |\lambda_5\rangle$, $|\lambda_3\rangle \leftrightarrow |\lambda_4\rangle$ are driven by the bath L, $|\lambda_6\rangle \leftrightarrow |\lambda_3\rangle$, $|\lambda_5\rangle \leftrightarrow |\lambda_2\rangle$, $|\lambda_4\rangle \leftrightarrow |\lambda_1\rangle$, $|\lambda_5\rangle \leftrightarrow |\lambda_4\rangle$, $|\lambda_2\rangle \leftrightarrow |\lambda_1\rangle$ are driven by the bath M, and $|\lambda_6\rangle \leftrightarrow |\lambda_2\rangle$, $|\lambda_6\rangle \leftrightarrow |\lambda_4\rangle$, $|\lambda_3\rangle \leftrightarrow |\lambda_1\rangle$ are driven by the bath R. Following the standard procedure [69], within the Born-Markovian approximation and the secular approximation, one can obtain the master equation in the Schrödinger picture as

$$\dot{\rho} = -i[H_S, \rho] + \mathcal{L}_L[\rho] + \mathcal{L}_M[\rho] + \mathcal{L}_R[\rho], \tag{8}$$

where the dissipator $\mathcal{L}_\mu[\rho]$ is given by

$$\begin{aligned} \mathcal{L}_\mu[\rho] = &\sum_l J_\mu(-\omega_{\mu l})[2V_{\mu l}(\omega_{\mu l})\rho V^\dagger_{\mu l}(\omega_{\mu l}) \\ &- \{V^\dagger_{\mu l}(\omega_{\mu l})V_{\mu l}(\omega_{\mu l}), \rho\}] \\ &+ J_\mu(+\omega_{\mu l})[2V^\dagger_{\mu l}(\omega_{\mu l})\rho V_{\mu l}(\omega_{\mu l}) \\ &- \{V_{\mu l}(\omega_{\mu l})V^\dagger_{\mu l}(\omega_{\mu l}), \rho\}], \end{aligned} \tag{9}$$

with the spectral densities defined by

$$J_\mu(+\omega_{\mu l}) = \gamma_\mu(\omega_{\mu l})n(\omega_{\mu l}), \tag{10}$$

$$J_\mu(-\omega_{\mu l}) = \gamma_\mu(\omega_{\mu l})[n(\omega_{\mu l})+1], \tag{11}$$

and the average photon number given by

$$n(\omega_{\mu l}) = \frac{1}{e^{\frac{\omega_{\mu l}}{T_\mu}}-1} \tag{12}$$

corresponding to the frequency $\omega_{\mu l}$ and the temperature T_μ. Due to the secular approximation, it requires $\gamma_\mu(\omega_{\mu l}) \ll \{|\omega_{\mu l} - \omega_{\mu l'} \pm 2g|, g\}$, which implies the strong internal coupling. In addition, we assume $\gamma_\mu(\omega_{\mu l}) = \gamma_\mu$ independent of the transition frequency for simplicity.

III. STEADY STATE OF THE OPEN SYSTEM AND THE HEAT CURRENTS

To demonstrate the functions of a thermal transistor, we need to study the steady-state thermal behavior of the open system. So the first key task is to find the steady solution of the master equation Eq. (8), namely, to solve $\dot{\rho}^S = 0$ [or Eq. (8) with $t \to \infty$]. To do so, we rewrite the master equation for the steady state as

$$\sum_{\mu=M,L,R} \mathbf{M}_\mu|\rho\rangle = 0, \quad \rho^S_{ij} = 0, i \neq j, \tag{13}$$

where $|\rho\rangle^T = [\rho^S_{11}, \rho^S_{22}, \rho^S_{33}, \rho^S_{44}, \rho^S_{55}, \rho^S_{66}]$ with

$$\begin{aligned}\mathbf{M}_L =& C_{2,1;3,2}\mathbf{J}_{L1}C^\dagger_{2,1;3,2} \\ &+ 2C_{5,1;6,2}\mathbf{J}_{L2}C^\dagger_{5,1;6,2} + C_{3,1;4,2}\mathbf{J}_{L3}C^\dagger_{3,1;4,2},\end{aligned} \tag{14}$$

$$\begin{aligned}\mathbf{M}_M =& 2C_{3,1;6,2}\mathbf{J}_{M1}C^\dagger_{3,1;6,2} \\ &+ C_{1,1;4,2}\mathbf{J}_{M2}C^\dagger_{1,1;4,2} + C_{2,1;5,2}\mathbf{J}_{M2}C^\dagger_{2,1;5,2} \\ &+ C_{1,1;2,2}\mathbf{J}_{M3}C^\dagger_{1,1;2,2} + C_{4,1;5,2}\mathbf{J}_{M3}C^\dagger_{4,1;5,2},\end{aligned} \tag{15}$$

$$\begin{aligned}\mathbf{M}_R =& C_{2,1;6,2}\mathbf{J}_{R1}C^\dagger_{2,1;6,2} \\ &+ C_{4,1;6,2}\mathbf{J}_{R2}C^\dagger_{4,1;6,2} + C_{1,1;3,2}\mathbf{J}_{R3}C^\dagger_{1,1;3,2}.\end{aligned} \tag{16}$$

Here $\mathbf{J}_{\mu l} = |2\rangle\langle 2| \otimes \begin{pmatrix} -A_{\mu l} & B_{\mu l} \\ A_{\mu l} & -B_{\mu l}\end{pmatrix}$ with $A_{\mu l} = \gamma_\mu(n(\omega_{\mu l})+1)$ and $B_{\mu l} = \gamma_\mu n(\omega_{\mu l})$, and $C_{i,j;m,n} = |i\rangle\langle j| + |m\rangle\langle n|$ with $\{|i\rangle\}$ representing the orthonormal basis of six-dimensional Hilbert space. One can find that Eq. (13) is analytically solvable, but the concrete expression is so tedious that it is impossible to present explicitly here. So we make some reasonable approximations in order to give an explicit presentation. Here all the involved parameters are taken as $E_1 = 4E$, $E_2 = 40E$, $E_3 = E_1 + E_2 = 44E$, $g = 0.75E_1$, $\gamma = 0.01E_1$, $T_L = 2E$, $T_R = 0.2E$, and $T_M < T_L$. Under this condition, the two higher energy levels $|\lambda_1\rangle$ and $|\lambda_4\rangle$ of H_S are difficult to excite, so one can easily check that the populations of ρ^S_{11} and ρ^S_{44} are much less than others, which can be seen from Figs. 2(a) and 2(b). This means that the contributions of these two energy levels $|\lambda_1\rangle$ and $|\lambda_4\rangle$ can be safely neglected to some good approximation.

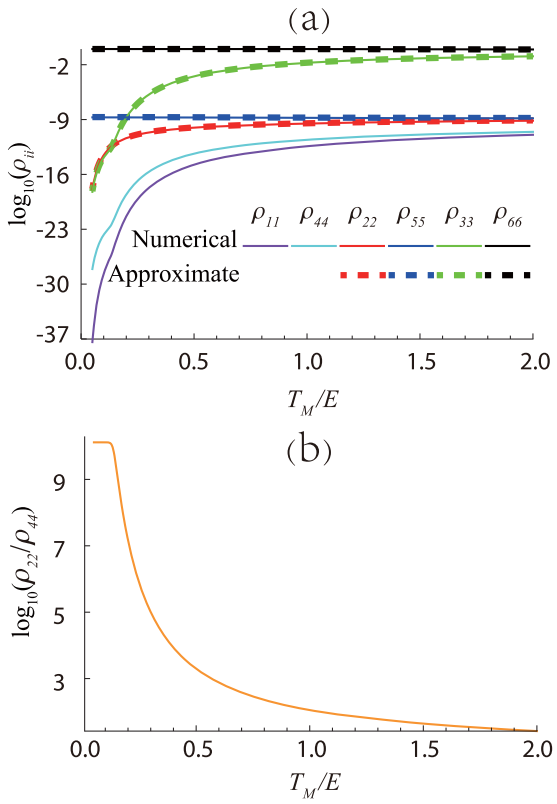

FIG. 2. (a) Numerical (solid lines) and approximate (dashed lines) populations versus T_M for the steady state. The lines from top to bottom at $T_M/E = 2$ correspond to ρ_{66}, ρ_{33}, ρ_{55}, ρ_{22}, ρ_{44}, and ρ_{11}. (b) The ratio ρ_{22}/ρ_{44} versus T_M for the steady state. Here $E_1 = 4E$, $E_2 = 40E$, $E_3 = E_1 + E_2 = 44E$, $g = 0.75E_1$, $\gamma = 0.01E_1$, $T_L = 2E$, and $T_R = 0.2E$. For both figures, one can find that ρ_{22} is less than ρ_{33}, ρ_{55}, and ρ_{66}, but ρ_{11} is less than ρ_{44}, which is much less than ρ_{22}. In this sense, ρ_{11} and ρ_{44} can be safely neglected to a good approximation.

Thus we can replace the irrelevant matrix entries in Eq. (13) by *zero*. In this way, the simplified Eq. (13) can be written as

$$\sum_{\mu=M,L,R} \tilde{\mathbf{M}}_\mu|\tilde{\rho}\rangle = 0, \quad \rho^S_{22} + \rho^S_{33} + \rho^S_{55} + \rho^S_{66} = 1, \tag{17}$$

where $\tilde{\mathbf{M}}_L = C_{2,1;3,2}\mathbf{J}_{L1}C^\dagger_{2,1;3,2} + 2C_{5,1;6,2}\mathbf{J}_{L2}C^\dagger_{5,1;6,2}$, $\tilde{\mathbf{M}}_M = 2C_{3,1;6,2}\mathbf{J}_{M1}C^\dagger_{3,1;6,2} + C_{1,1;4,2}\mathbf{J}_{M2}C^\dagger_{1,1;4,2} + C_{2,1;5,2}\mathbf{J}_{M2}C^\dagger_{2,1;5,2}$, $\tilde{\mathbf{M}}_R = C_{2,1;6,2}\mathbf{J}_{R1}C^\dagger_{2,1;6,2}$, and $|\tilde{\rho}\rangle = [0, \rho^S_{22}, \rho^S_{33}, 0, \rho^S_{55}, \rho^S_{66}]^T$. As a result, one can obtain

$$\rho^S_{22} = \frac{D_2}{D}, \quad \rho^S_{33} = \frac{D_3}{D}, \quad \rho^S_{55} = \frac{D_5}{D}, \quad \rho^S_{66} = \frac{D_6}{D}, \tag{18}$$

where

$$\begin{aligned}D_2 =& 2A_{L2}[2B_{M1}B_{L1} + B_{R1}(2A_{M1} + B_{L1})] + B_{M2} \\ &\times [2B_{M1}B_{L1} + (2A_{M1} + B_{L1})(2B_{L2} + B_{R1})],\end{aligned} \tag{19}$$

$$\begin{aligned}D_3 =& 2B_{M1}[2A_{M2}A_{L2} + A_{R1}(2A_{L2} + B_{M2})] + A_{L1} \\ &\times [2A_{L2}(2B_{M1} + B_{R1}) \\ &+ B_{M2}(2B_{M1} + 2B_{L2} + B_{R1})],\end{aligned} \tag{20}$$

$$D_5 = 2B_{L2}[A_{R1}B_{L1} + 2A_{M1}(A_{L1} + A_{R1})] + A_{M2} \times [2B_{M1}B_{L1} + (2A_{M1} + B_{L1})(2B_{L2} + B_{R1})], \quad (21)$$

$$D_6 = B_{L1}[2A_{M2}A_{L2} + A_{R1}(2A_{L2} + B_{M2})] + 2A_{M1} \times [2A_{M2}A_{L2} + (A_{L1} + A_{R1})(2A_{L2} + B_{M2})],$$

$$D = D_2 + D_3 + D_5 + D_6. \quad (22)$$

With the solutions of Eq. (18), one can calculate the heat currents subject to different baths as [23,70–72]

$$\dot{Q}_\mu = Tr(H_S \mathcal{L}_\mu[\rho^S]) \approx \langle\lambda|\tilde{\mathbf{M}}_\mu|\tilde{\rho}\rangle, \quad (23)$$

which can be explicitly given by

$$\dot{Q}_L = -\omega_{L1}\Gamma^L_{23} - 2\omega_{L2}\Gamma^L_{56}, \quad (24)$$

$$\dot{Q}_M = -2\omega_{M1}\Gamma^M_{36} - \omega_{M2}\Gamma^M_{25}, \quad (25)$$

$$\dot{Q}_R = -\omega_{R1}\Gamma^R_{26}, \quad (26)$$

where

$$\Gamma^\mu_{i,j} = \gamma_\mu\left[(n_\mu(\lambda_i - \lambda_j) + 1)\rho^S_{ii} - n_\mu(\lambda_i - \lambda_j)\rho^S_{jj}\right] \quad (27)$$

denotes the net decay rate from the state $|i\rangle$ to $|j\rangle$ due to the coupling with the μth bath. One knows that $\dot{Q}_\mu > 0$ means the heat flows out of the μth bath and $\dot{Q}_\mu < 0$ corresponds to the heat flows into the μth bath. It can be easily checked that $\dot{Q}_L + \dot{Q}_M + \dot{Q}_R = 0$ corresponding to the energy conservation law. In the next section, we will show that the heat currents can be effectively controlled, and hence our thermal device can realize the functions of a thermal transistor.

IV. THE FUNCTIONS AS A TRANSISTOR

Now we will show that the weak *modulation* heat current $\dot{Q}_M$ can modulate, switch, and stabilize the output currents through the *target* qutrit; moreover, our model can realize the typical function as a thermal transistor—the amplification of the weak *modulation* heat current $\dot{Q}_M$, i.e., the left current $\dot{Q}_L$ or the right one $\dot{Q}_R$ can become greatly larger than $\dot{Q}_M$ with a dynamical amplification factor α defined as

$$\alpha_{L,R} = \frac{\partial \dot{Q}_{L,R}}{\partial \dot{Q}_M}. \quad (28)$$

If the amplification factor $\alpha_{L,R} > 1$, we can say the transistor effect is achieved. In particular, the larger $\alpha_{L,R}$ is, the better a transistor effect is obtained.

Switch—In order to show the function as a quantum thermal switch, we plot the three heat currents in Fig. 3. It is obvious that all three heat currents are very small and even close to zero in the low-temperature T_M regime, i.e., $T_M/E \lesssim 0.3$. Especially $\dot{Q}_{L,R}$ in the low-temperature T_M regime are much smaller than those in the large T_M regime. Therefore, if the heat currents are neglectfully small, we can think that the heat conduction is prevented between the bath L and the bath R. In this sense, one can find that our model can be considered to be at the "*off*" state for $T_M/E \lesssim 0.3$. With the increase of T_M, the heat currents $\dot{Q}_{L,R}$ are gradually increased, namely, the switch is gradually open and the heat is allowed to transport between the bath L and the bath R. It is especially noted that if the switch is off, T_M can be taken in a large safe range so long as $T_M/E \lesssim 0.3$ is satisfied. Actually, one can always define an exact critical small value of the allowable heat current based on the practical case. When the heat current value is less than this critical value, one can think the switch is off, and when the heat current is larger than the critical value, the switch is on.

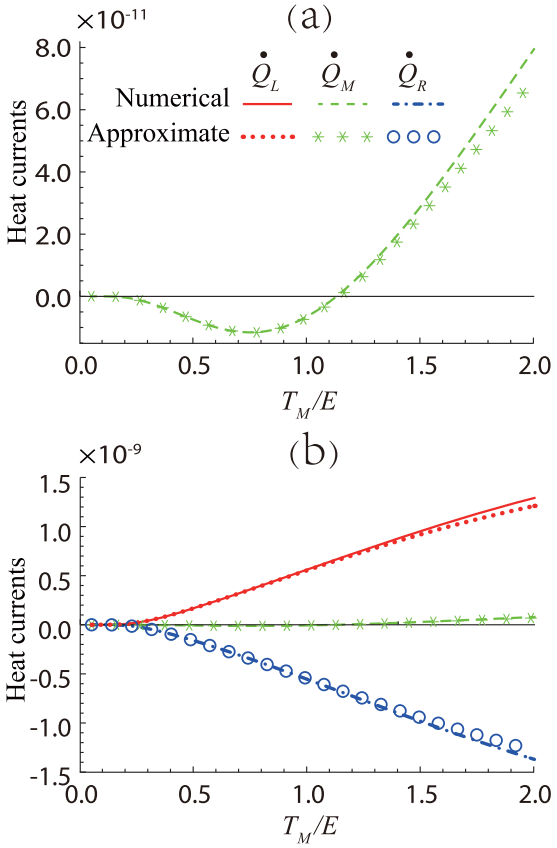

FIG. 3. Three thermal currents $\dot{Q}_L$, $\dot{Q}_M$, and $\dot{Q}_R$ via numerical and approximate methods at steady state versus T_M. The parameters are the same as in Fig. 2.

Modulation—The modulation function means the heat current can be controlled continuously from a small value to a large one by another much smaller continuous current. From Fig. 3, one can find that in the whole range of T_M, $\dot{Q}_M$ always keeps much smaller than $\dot{Q}_{L,R}$, while $\dot{Q}_{L,R}$ ranges from a small value (can reach zero) at low T_M to a large one for a large T_M. In this perspective, the two currents $\dot{Q}_{L,R}$ are modulated by a tiny modulation current $\dot{Q}_M$, and the modulation function is realized.

Amplification—The crucial feature of a transistor is the function of amplification; namely, the weak modulation heat current $\dot{Q}_M$ amplifies (or induces) a strong heat current which transports between the bath L and the bath R. In fact, it is apparent that from Fig. 3 that the current $\dot{Q}_M$ varies gently when $0.3 \lesssim T_M/E$, but the currents $\dot{Q}_{L,R}$ are changed rapidly, which implies the amplification is achieved. However, in order to precisely describe the amplification effect, one has to employ the amplification factor α defined in Eq. (28). In Fig. 4, we present the two amplification factors α_L and α_R versus T_M. The two amplification factors are obviously larger than 1, which shows that the amplification effect indeed exits in our model. At

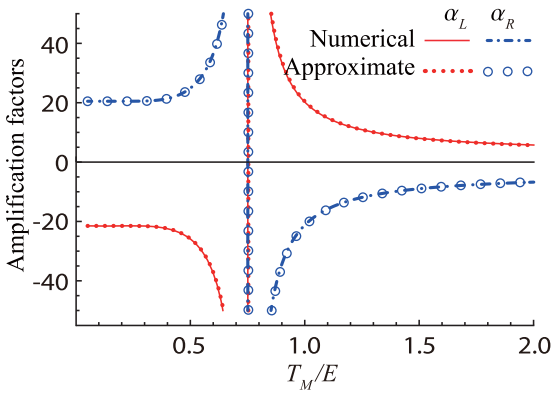

FIG. 4. Two amplification factors α_L and α_R via numerical and approximate methods at steady state versus T_M. The parameters are the same as in Fig. 2.

the low-temperature range $0 < T_M/E < 0.5$, the heat current is stably amplified due to almost the same amplification factors (about 20). At the range $0.5 < T_M/E < 1$, the amplification factors strongly depend on the temperature T_M. This can be regarded as a sensitive region, which means a tiny change of the modulation current $\dot{Q}_M$ can lead to the drastic change of the currents $\dot{Q}_{L,R}$. The region $T_M/E > 1$ can be considered as the weak stable amplification region. But the factors $\alpha_{L,R}$ are still larger than 1, for example, $\alpha_L = 5.749$ and $\alpha_R = -6.749$ for $T_M/E = 2.0$. Thus, one can select the proper working region based on what kind of amplification is required in the practical scenario.

Stabilizer—In fact, our model can also work for a stabilizer of heat currents; namely, the heat currents $\dot{Q}_{L,R}$ are not sensitive to the change of temperature of T_R (the low-temperature terminal). To illustrate such a function, we plot the three heat currents versus T_R in Fig. 5. One can see that when the temperature T_R varies from 0 to about T_R along the horizontal axis, the heat currents $\dot{Q}_{L,R}$ are kept almost in the horizontal lines, i.e., there is no obvious change of the heat currents $\dot{Q}_{L,R}$. In fact, a direct understanding of this phenomenon can be obtained by our Eqs. (26) and (27) where the fluctuation of the lower temperature at the R terminal subject to the large transition frequency between the energy levels $|\lambda_2\rangle$ and $|\lambda_6\rangle$ cannot lead to the considerable fluctuation of the net decay rate.

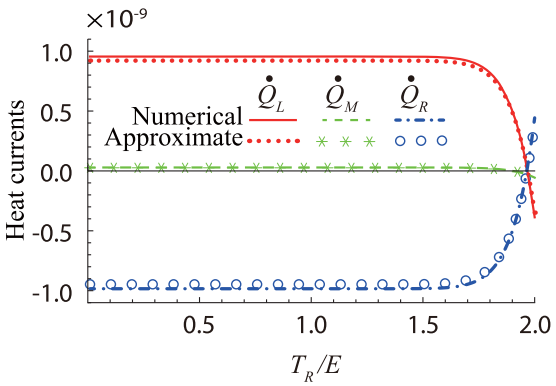

FIG. 5. Three thermal currents $\dot{Q}_L$, $\dot{Q}_M$, and $\dot{Q}_R$ via numerical and approximate methods at steady state versus T_R. Here $T_M/E = 1.5$ and the parameters are the same as in Fig. 2.

In other words, the large fluctuations of T_R cannot drastically influence the heat currents $\dot{Q}_{L,R}$; namely, $\dot{Q}_{L,R}$ in the given temperature range are stabilized.

Finally, we emphasize that the thermal transistor proposed in this paper is a thermal device with three terminals. Here we use the heat Q_M as the "modulation" terminal which controls the heat currents between the other two terminals. What we would like to emphasize is that the choice of the "modulation" terminal is not unique. In Appendix B, we have numerically studied the cases with Q_L and Q_R as the "modulation" terminal. It is shown that in both cases our proposed thermal device can realize all the mentioned functions as a transistor including the functions of the switch, the modulation, and the amplification. As to the function of the stabilizer, one can also find that if the heat current Q_L is the low-temperature terminal, the heat currents $Q_{L,R}$ can also be stabilized. In fact, throughout the paper, we intend to fix T_M as a medium temperature between T_L and T_R, which is enough for us to show our device is a transistor. If other parameters are selected, one can find that the function as a transistor can be realized in different cases which are not indicated extensively. We also consider the case of the weak internal coupling. One can find that the transistor effect still exists, but the price is that the heat currents will be reduced to a very low level (too small). This actually coincides with Refs. [38,39] working in the cooling regime, where the strong internal coupling suppresses the cooling, but the current model works in the heating regime. An intuitive understanding could be that the suppression of cooling implies the enhancement of heating. In addition, one can also find that compared with Ref. [60], we have realized similar functions with fewer energy levels and particles with a different mechanism.

V. DISCUSSION AND CONCLUSION

Before concluding, we would like to give some discussion about the potential design in superconducting systems. As we know, a superconducting artificial atom provides the possibility to realize a Δ-type system allowing different transitions between the three levels [65,66]. One distinct advantage is that the energy gap can be customized freely, for instance, via changing the magnetic flux in a circuit QED architecture, and another advantage is that the coupling between the superconducting artificial atoms can be easily tuned to be strong [73,74]. The energy gap of superconducting circuits ranges from 1 to 10 GHz or even higher, and the strong coupling is about the order of 1 GHz via mutual inductance or capacitance. The choice of the coupling energy levels is well guaranteed by the rotating wave approximation so long as the large detuning is adjusted. The coupling between the system and a bath can be achieved via a resonator, and a resistor acts as a bath [68,75]. In fact, the reservoir could be directly tailored with the desired bath spectra by reservoir engineering, which has been described in detail and applied in many cases [43,76–78]. In addition, one can note that autonomous quantum refrigerator in a circuit QED architecture based on a Josephson junction and a quantum heat switch based on coupled superconducting qubits have been proposed in Refs. [67,68], and other relevant investigations about heat transport can also be found in their references.

In conclusion, we have presented a thermal device to realize the functions of a thermal transistor by utilizing the strong internal coupling between the qubit and the qutrit, which are connected to three baths with different temperatures. We mainly emphasize the functions as the thermal switch, the modulation, the stabilization, and the amplification, which are rigorously demonstrated by both the numerical and the approximately analytic procedures. It is shown that the adjustable energy levels in the qutrit system play a significant role in the design of the thermal transistor. We also present a possible experimental scheme to realize the concept.

ACKNOWLEDGMENTS

This work was supported by the National Natural Science Foundation of China, under Grants No. 11775040 and No. 11375036, the Xinghai Scholar Cultivation Plan, and the Fundamental Research Fund for the Central Universities under Grant No. DUT18LK45.

APPENDIX A: EIGENOPERATORS OF THE SYSTEM

In order to derive the master equation, we would like to emphasize that the Born-Markov approximation and secular approximation will be used following the standard procedure [69]. We also require a large internal coupling g to satisfy the secular approximation condition. Considering the total Hamiltonian including the three baths as

$$H = H_S + H_{SB} + \sum_{\mu} H_{\mu}, \tag{A1}$$

we can first diagonalize the Hamiltonian H_S and then in the H_S representation derive the eigenoperators with their corresponding eigenfrequencies $\omega_{\mu l}$ as

$$V_{L1} = \frac{1}{\sqrt{2}}(|\lambda_3\rangle\langle\lambda_2|), \quad \omega_{L1} = E_2 - g, \tag{A2}$$

$$V_{L2} = |\lambda_6\rangle\langle\lambda_5|, \quad \omega_{L2} = E_2, \tag{A3}$$

$$V_{L3} = \frac{1}{\sqrt{2}}(|\lambda_3\rangle\langle\lambda_4|), \quad \omega_{L3} = E_2 + g, \tag{A4}$$

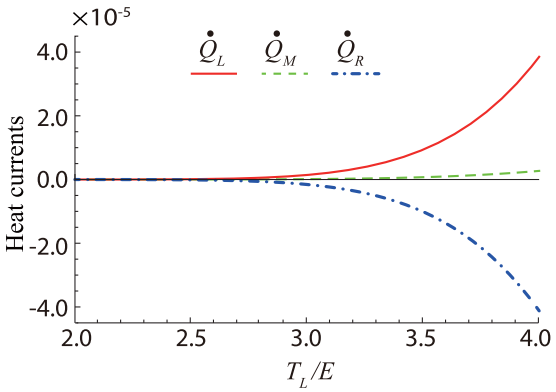

FIG. 6. Three thermal currents $\dot{Q}_L$, $\dot{Q}_M$, and $\dot{Q}_R$ via numerical method at steady state versus T_L. Here $T_M/E = 4$, $T_R/E = 2$, and the other parameters are the same as in Fig. 2.

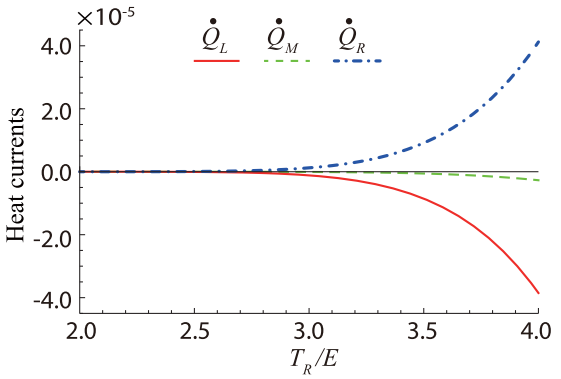

FIG. 7. Three thermal currents $\dot{Q}_L$, $\dot{Q}_M$, and $\dot{Q}_R$ via numerical method at steady state versus T_R. Here $T_M/E = 4$, $T_L/E = 2$, and the other parameters are the same as in Fig. 2.

$$V_{M1} = |\lambda_6\rangle\langle\lambda_3|, \quad \omega_{M1} = E_1, \tag{A5}$$

$$V_{M2} = \frac{1}{\sqrt{2}}(|\lambda_5\rangle\langle\lambda_2| + |\lambda_4\rangle\langle\lambda_1|), \quad \omega_{M2} = E_1 - g, \tag{A6}$$

$$V_{M3} = \frac{1}{\sqrt{2}}(|\lambda_5\rangle\langle\lambda_4| - |\lambda_2\rangle\langle\lambda_1|), \quad \omega_{M3} = E_1 + g, \tag{A7}$$

$$V_{R1} = \frac{1}{\sqrt{2}}(|\lambda_6\rangle\langle\lambda_2|), \quad \omega_{R1} = E_3 - g, \tag{A8}$$

$$V_{R2} = -\frac{1}{\sqrt{2}}(|\lambda_6\rangle\langle\lambda_4|), \quad \omega_{R2} = E_3 + g, \tag{A9}$$

$$V_{R3} = |\lambda_3\rangle\langle\lambda_1|, \quad \omega_{R3} = E_3. \tag{A10}$$

The master equation can be directly obtained by substituting these eigenoperators into the standard Lindbladian master equation:

$$\frac{d\rho_S}{dt} = -i[H_S, \rho_S] + \sum_{k=1}^{N^2-1} \gamma_k \left(A_k \rho_S A_k^{\dagger} - \frac{1}{2} A_k^{\dagger} A_k \rho_S - \frac{1}{2} \rho_S A_k^{\dagger} A_k \right). \tag{A11}$$

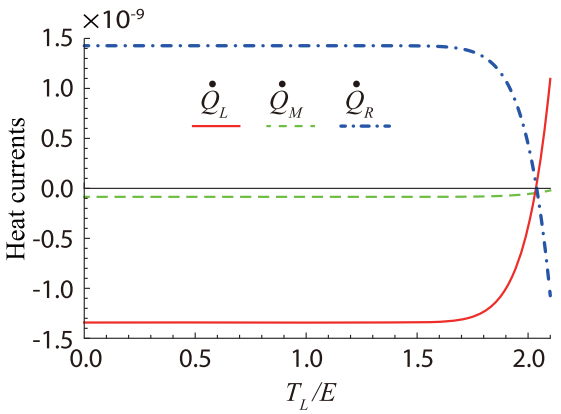

FIG. 8. Three thermal currents $\dot{Q}_L$, $\dot{Q}_M$, and $\dot{Q}_R$ via numerical method at steady state versus T_L. Here $T_M/E = 1.5$, $T_R/E = 2$, and the other parameters are the same as in Fig. 2.

What we should pay attention to is the formula for γ. The master equation for our model can be found in the main text; we will not show it here again.

APPENDIX B: THE TRANSISTOR WITH DIFFERENT MODULATION TERMINALS

In the main text, we consider $\dot{Q}_M$ as the modulation current, which can effectively control the heat current between the other two terminals. Here we will show that $\dot{Q}_{L/R}$ can also be used as the modulation current, which is explicitly illustrated in Figs. 6 and 7. It is obvious that the functions of interests like the switch, the modulation, and the amplification can be realized in the different parameter ranges. In addition, in Fig. 8 we plot the function of the heat current stabilization subject to the temperature fluctuation at the terminal L. Although a different lower-temperature terminal is used in contrast to the main text, the heat currents are robust only to the temperature fluctuation of the lower-temperature terminal.

[1] V. E. Lashkaryov, Investigations of a barrier layer by the thermoprobe method, Izv. Akad. Nauk SSSR, Ser. Fiz. **5**, 422 (1941).

[2] J. Bardeen and W. H. Brattain, The transistor, a semiconductor triode, Proc. IEEE **86**, 29 (1998).

[3] C. W. Chang, D. Okawa, A. Majumdar, and A. Zettl, Solid-state thermal rectifier, Science **314**, 1121 (2006).

[4] R. Scheibner, M. König, D. Reuter, A. D. Wieck, C. Gould, H. Buhmann, and L. W. Molenkamp, Quantum dot as thermal rectifier, New J. Phys. **10**, 083016 (2008).

[5] W. Kobayashi, Y. Teraoka, and I. Terasaki, An oxide thermal rectifier, Appl. Phys. Lett. **95**, 171905 (2009).

[6] P. J. van Zwol, L. Ranno, and J. Chevrier, Tuning Near Field Radiative Heat Flux through Surface Excitations with a Metal Insulator Transition, Phys. Rev. Lett. **108**, 234301 (2012).

[7] P. J. van Zwol, L. Ranno, and J. Chevrier, Emissivity measurements with an atomic force microscope, J. Appl. Phys. **111**, 063110 (2012).

[8] K. Ito, K. Nishikawa, and H. Iizuka, Multilevel radiative thermal memory realized by the hysteretic metal-insulator transition of vanadium dioxide, Appl. Phys. Lett. **108**, 053507 (2016).

[9] P. Ben-Abdallah and S. A. Biehs, Phase-change radiative thermal diode, Appl. Phys. Lett. **103**, 191907 (2013).

[10] Y. Yang, S. Basu, and L. P. Wang, Radiation-based near-field thermal rectification with phase transition materials, Appl. Phys. Lett. **103**, 163101 (2013).

[11] K. Ito, K. Nishikawa, H. Iizuka, and H. Toshiyoshi, Experimental investigation of radiative thermal rectifier using vanadium dioxide, Appl. Phys. Lett. **105**, 253503 (2014).

[12] P. Ben-Abdallah and S. A. Biehs, Near-Field Thermal Transistor, Phys. Rev. Lett. **112**, 044301 (2014).

[13] K. Joulain, Y. Ezzahri, J. Drevillon, and P. Ben-Abdallah, Modulation and amplification of radiative far field heat transfer: Towards a simple radiative thermal transistor, Appl. Phys. Lett. **106**, 133505 (2015).

[14] L. Wang, B. Hu, and B. W. Li, Validity of Fourier's law in one-dimensional momentum-conserving lattices with asymmetric interparticle interactions, Phys. Rev. E **88**, 052112 (2013).

[15] G. T. Landi and M. J. de Oliveira, Fourier's law from a chain of coupled anharmonic oscillators under energy-conserving noise, Phys. Rev. E **87**, 052126 (2013).

[16] C. W. Chang, D. Okawa, H. Garcia, A. Majumdar, and A. Zettl, Breakdown of Fourier's Law in Nanotube Thermal Conductors, Phys. Rev. Lett. **101**, 075903 (2008).

[17] D. Manzano, M. Tiersch, A. Asadian, and H. J. Briegel, Quantum transport efficiency and Fourier's law, Phys. Rev. E **86**, 061118 (2012).

[18] Y. Zhang and H. Zhao, Heat conduction in a one-dimensional aperiodic system, Phys. Rev. E **66**, 026106 (2002).

[19] J. W. Mao, Y. Q. Li, and Y. Y. Ji, Role of chaos in one-dimensional heat conductivity, Phys. Rev. E **71**, 061202 (2005).

[20] B. Hu, D. He, L. Yang, and Y. Zhang, Asymmetric heat conduction through a weak link, Phys. Rev. E **74**, 060101 (2006).

[21] A. Levy and R. Kosloff, The local approach to quantum transport may violate the second law of thermodynamics, Europhys. Lett. **107**, 20004 (2014).

[22] P. T. Landsberg, Foundations of thermodynamics, Rev. Mod. Phys. **28**, 363 (1956).

[23] A. Levy, R. Alicki, and R. Kosloff, Quantum refrigerators and the third law of thermodynamics, Phys. Rev. E **85**, 061126 (2012).

[24] K. Maruyama, F. Nori, and V. Vedral, Colloquium: The physics of Maxwell's demon and information, Rev. Mod. Phys. **81**, 1 (2009).

[25] T. Feldmann and R. Kosloff, Performance of discrete heat engines and heat pumps in finite time, Phys. Rev. E **61**, 4774 (2000).

[26] J. P. Palao, R. Kosloff, and J. M. Gordon, Quantum thermodynamic cooling cycle, Phys. Rev. E **64**, 056130 (2001).

[27] J. Arnaud, L. Chusseau, and F. Philippe, Carnot cycle for an oscillator, Eur. J. Phys. **23**, 489 (2002).

[28] D. Segal and A. Nitzan, Molecular heat pump, Phys. Rev. E **73**, 026109 (2006).

[29] C. de Tomás, A. C. Hernández, and J. M. M. Roco, Optimal low symmetric dissipation Carnot engines and refrigerators, Phys. Rev. E **85**, 010104 (2012).

[30] E. Geva and R. Kosloff, A quantum-mechanical heat engine operating in finite time: A model consisting of spin-1/2 systems as the working fluid, J. Chem. Phys. **96**, 3054 (1992).

[31] E. Geva and R. Kosloff, The quantum heat engine and heat pump: An irreversible thermodynamic analysis of the three-level amplifier, J. Chem. Phys. **104**, 7681 (1996).

[32] R. Kosloff and T. Feldmann, Optimal performance of reciprocating demagnetization quantum refrigerators, Phys. Rev. E **82**, 011134 (2010).

[33] G. Thomas and R. S. Johal, Coupled quantum Otto cycle, Phys. Rev. E **83**, 031135 (2011).

[34] T. Feldmann, E. Geva, R. Kosloff, and P. Salamon, Heat engines in finite time governed by master equations, Am. J. Phys. **64**, 485 (1996).

[35] T. Feldmann and R. Kosloff, Quantum four-stroke heat engine: Thermodynamic observables in a model with intrinsic friction, Phys. Rev. E **68**, 016101 (2003).

[36] H. T. Quan, Y. X. Liu, C. P. Sun, and F. Nori, Quantum thermodynamic cycles and quantum heat engines, Phys. Rev. E **76**, 031105 (2007).
[37] N. Linden, S. Popescu, and P. Skrzypczyk, How Small Can Thermal Machines Be? The Smallest Possible Refrigerator, Phys. Rev. Lett. **105**, 130401 (2010).
[38] C. S. Yu and Q. Y. Zhu, Re-examining the self-contained quantum refrigerator in the strong-coupling regime, Phys. Rev. E **90**, 052142 (2014).
[39] Z.-X. Man and Y.-J. Xia, Smallest quantum thermal machine: The effect of strong coupling and distributed thermal tasks, Phys. Rev. E **96**, 012122 (2017).
[40] R. Silva, P. Skrzypczyk, and N. Brunner, Small quantum absorption refrigerator with reversed couplings, Phys. Rev. E **92**, 012136 (2015).
[41] O. Abah, J. Roßnagel, G. Jacob, S. Deffner, F. Schmidt-Kaler, K. Singer, and E. Lutz, Single-Ion Heat Engine at Maximum Power, Phys. Rev. Lett. **109**, 203006 (2012).
[42] J. Roßnagel, S. T. Dawkins, K. N. Tolazzi, O. Abah, E. Lutz, F. Schmidt-Kaler, and K. Singer, A single-atom heat engine, Science **352**, 325 (2016).
[43] H. E. D. Scovil and E. O. Schulz-DuBois, Three-Level Masers as Heat Engines, Phys. Rev. Lett. **2**, 262 (1959).
[44] R. Alicki, The quantum open system as a model of the heat engine, J. Phys. A **12**, L103 (1979).
[45] P. Skrzypczyk, N. Brunner, N. Linden, and S. Popescu, The smallest refrigerators can reach maximal efficiency, J. Phys. A **44**, 492002 (2011).
[46] L. Wang and B. W. Li, Thermal Logic Gates: Computation with Phonons, Phys. Rev. Lett. **99**, 177208 (2007).
[47] L. Wang and B. W. Li, Thermal Memory: A Storage of Phononic Information, Phys. Rev. Lett. **101**, 267203 (2008).
[48] L. P. Faucheux, L. S. Bourdieu, P. D. Kaplan, and A. J. Libchaber, Optical Thermal Ratchet, Phys. Rev. Lett. **74**, 1504 (1995).
[49] F. Zhan, N. B. Li, S. Kohler, and P. Hänggi, Molecular wires acting as quantum heat ratchets, Phys. Rev. E **80**, 061115 (2009).
[50] P. P. Hofer, J. B. Brask, M. Perarnau-Llobet, and N. Brunner, Quantum Thermal Machine as a Thermometer, Phys. Rev. Lett. **119**, 090603 (2017).
[51] T. Werlang, M. A. Marchiori, M. F. Cornelio, and D. Valente, Optimal rectification in the ultrastrong coupling regime, Phys. Rev. E **89**, 062109 (2014).
[52] T. Chen and X. B. Wang, Thermal rectification in the nonequilibrium quantum-dots-system, Physica E **72**, 58 (2015).
[53] B. W. Li, L. Wang, and G. Casati, Thermal Diode: Rectification of Heat Flux, Phys. Rev. Lett. **93**, 184301 (2004).
[54] E. Pereira, Sufficient conditions for thermal rectification in general graded materials, Phys. Rev. E **83**, 031106 (2011).
[55] J. Wang, E. Pereira, and G. Casati, Thermal rectification in graded materials, Phys. Rev. E **86**, 010101 (2012).
[56] F. Fratini and R. Ghobadi, Full quantum treatment of a light diode, Phys. Rev. A **93**, 023818 (2016).
[57] G. T. Landi, E. Novais, M. J. de Oliveira, and D. Karevski, Flux rectification in the quantum XXZ chain, Phys. Rev. E **90**, 042142 (2014).
[58] Z. X. Man, N. B. An, and Y. J. Xia, Controlling heat flows among three reservoirs asymmetrically coupled to two two-level systems, Phys. Rev. E **94**, 042135 (2016).
[59] J. H. Jiang, M. Kulkarni, D. Segal, and Y. Imry, Phonon thermoelectric transistors and rectifiers, Phys. Rev. B **92**, 045309 (2015).
[60] K. Joulain, J. Drevillon, Y. Ezzahri, and J. Ordonez-Miranda, Quantum Thermal Transistor, Phys. Rev. Lett. **116**, 200601 (2016).
[61] W. C. Lo, L. Wang, and B. W. Li, Thermal transistor: Heat flux switching and modulating, J. Phys. Soc. Jpn. **77**, 054402 (2008).
[62] B. W. Li, L. Wang, and G. Casati, Negative differential thermal resistance and thermal transistor, Appl. Phys. Lett. **88**, 143501 (2006).
[63] T. S. Komatsu and N. Ito, Thermal transistor utilizing gas-liquid transition, Phys. Rev. E **83**, 012104 (2011).
[64] K. Joulain, Y. Ezzahri, and J. Ordonez-Miranda, Quantum thermal rectification to design thermal diodes and transistors, Z. Naturforsch. A **72**, 163 (2017).
[65] J. Q. You and F. Nori, Atomic physics and quantum optics using superconducting circuits, Nature (London) **474**, 589 (2011).
[66] I. Buluta, S. Ashhab, and F. Nori, Natural and artificial atoms for quantum computation, Rep. Prog. Phys. **74**, 104401 (2011).
[67] P. P. Hofer, M. Perarnau-Llobet, J. B. Brask, R. Silva, M. Huber, and N. Brunner, Autonomous quantum refrigerator in a circuit QED architecture based on a Josephson junction, Phys. Rev. B **94**, 235420 (2016).
[68] B. Karimi, J. P. Pekola, M. Campisi, and R. Fazio, Coupled qubits as a quantum heat switch, Quantum Sci. Tech. **2**, 044007 (2017).
[69] H. P. Breuer and F. Petruccione, *The Theory of Open Quantum Systems* (Oxford University Press, Oxford, 2002).
[70] K. Szczygielski, D. Gelbwaser-Klimovsky, and R. Alicki, Markovian master equation and thermodynamics of a two-level system in a strong laser field, Phys. Rev. E **87**, 012120 (2013).
[71] R. Alicki, D. A. Lidar, and P. Zanardi, Internal consistency of fault-tolerant quantum error correction in light of rigorous derivations of the quantum Markovian limit, Phys. Rev. A **73**, 052311 (2006).
[72] M. Kolář, D. Gelbwaser-Klimovsky, R. Alicki, and G. Kurizki, Quantum Bath Refrigeration Towards Absolute Zero: Challenging the Unattainability Principle, Phys. Rev. Lett. **109**, 090601 (2012).
[73] A. O. Niskanen, K. Harrabi, F. Yoshihara, Y. Nakamura, S. Lloyd, and J. S. Tsai, Quantum coherent tunable coupling of superconducting qubits, Science **316**, 723 (2007).
[74] T. Hime, P. A. Reichardt, B. L. T. Plourde, T. L. Robertson, C.-E. Wu, A. V. Ustinov, and J. Clarke, Solid-state qubits with current-controlled coupling, Science **314**, 1427 (2006).
[75] N. Cottet, S. Jezouin, L. Bretheau, P. Campagne-Ibarcq, Q. Ficheux, J. Anders, A. Auffèves, R. Azouit, P. Rouchon, and B. Huard, Observing a quantum Maxwell demon at work, Proc. Natl. Acad. Sci. USA **114**, 7561 (2017).
[76] D. Gelbwaser-Klimovsky, R. Alicki, and G. Kurizki, Minimal universal quantum heat machine, Phys. Rev. E **87**, 012140 (2013).
[77] C. J. Myatt, B. E. King, Q. A. Turchette, C. A. Sackett, D. Kielpinski, W. M. Itano, C. Monroe, and D. J. Wineland, Decoherence of quantum superpositions through coupling to engineered reservoirs, Nature (London) **403**, 269 (2000).
[78] S. Gröblacher, A. Trubarov, N. Prigge, G. D. Cole, M. Aspelmeyer, and J. Eisert, Observation of non-Markovian micromechanical Brownian motion, Nat. Commun. **6**, 7606 (2015).